

Physical Properties of Polyamide 6/H-NBR Blends and the Effects of Dynamic Vulcanization on Them

S. W. Hwang,^{1,2} S. W. Kim,³ H. Y. Park,⁴ I. L. Jeon,⁵ K. H. Seo⁴

¹School of Packaging, Michigan State University, East Lansing, Michigan 48824

²Korea Packaging Center, Korea Institute of Industrial Technology, Bucheon-si, South Korea

³Korean Intellectual Property Office, Daejeon, South Korea

⁴Department of Polymer Science, Kyungpook National University, Daegu, South Korea

⁵School of Fire and Disaster Prevention, Kyungil University, Gyeongsan-si, South Korea

Received 15 July 2009; accepted 2 January 2010

DOI 10.1002/app.33044

Published online 24 September 2010 in Wiley Online Library (wileyonlinelibrary.com).

ABSTRACT: Polyamide 6 (PA 6) and hydrogenated nitrile rubber (H-NBR) were blended with various blend ratios in a brabender plasticoder at 240°C/100 rpm. The processing characteristics with a mixing torque of the blends were investigated. The effect of the blend ratio on physical properties such as tensile strength, Young's modulus, elongation at break, permanent set, hardness, and swelling behavior of blends was analyzed. Most mechanical properties were found to decrease with an addition of H-NBR. The morphology of the blends was observed, and the results show a two phase system where the component with high proportions exists as a continuous phase. A

cocontinuous phase was observed in blend ratios of 50/50 and 40/60. Dynamic mechanical properties were observed to study a viscoelastic property of the blends. In addition, the effect of dynamic vulcanization with peroxide on physical properties was studied, and the influence of peroxide on PA 6 was also examined. It was found that the peroxide can have an effect on PA 6 as well as act as a crosslinker to H-NBR. © 2010 Wiley Periodicals, Inc. *J Appl Polym Sci* 119: 3136–3144, 2011

Key words: blends; polyamide 6; H-NBR; dynamic vulcanization

INTRODUCTION

Polymer blends have gained importance for many years, because the blending with two polymers gives rise to enhanced physical properties for specific application.^{1,2} Most of the polymer blends are found to be an immiscible system. These immiscible system blends are characterized by a two-phase morphology, poor physical, and chemical interactions across the phase boundaries and poor mechanical properties.^{3,4} Dynamic vulcanization of polymer blends was found to improve the properties of immiscible polymer blends by providing stable morphology and good interfacial adhesion.^{5–8}

Thermoplastic elastomers (TPE) have undergone an extensive growth in production with the success in commercialization over the past two decades.⁹ TPE can be block copolymers, which contain rubber and resinous molecular systems, such as styrene-butadiene-styrene triblock copolymer¹⁰ and ester or ether-urethane alternating block copolymers,¹¹ or they can be blends of a rubber–plastic combination such as crystalline polyolefine–ethylene–propylene–

diene monomer. In the recent years, TPE prepared from rubber–plastic blends have gained great importance due to their excellent processability and rubberlike behavior at ambient temperature.^{12–15}

Dynamic vulcanization was first described by Gessler¹⁶ in 1962 and then developed by Fisher¹⁷ and Coran et al.¹⁸ It is the process of vulcanizing an elastomer during its melt-mixing with a molten plastic. Dynamic vulcanization is a method to develop new TPE, which has many properties as good as those of elastomeric block copolymers. This technology has led to a significant number of new thermoplastic elastomeric products commercialized during late 1980s.¹⁹ Some TPE through dynamic vulcanization has been commercialized with trade names such as Santoprene and Geolast.²⁰

Polyamide 6 (PA 6) is used to blend with amorphous polymers such as rubbers due to its high modulus, good mechanical strength, thermal stability, and chemical resistance.^{21–24} Nitrile rubber (NBR) is a rubber having good oil resistance due to the presence of the polar acrylonitrile group, but it cannot be used at elevated temperatures above 100°C. Hydrogenated acrylonitrile rubber (H-NBR) received special attention because of remarkable stability in hydrocarbons and has higher resistance at elevated temperatures (about 150°C).^{25,26} In this study, the physical properties of the blends with PA 6 and H-NBR were investigated, and the effect of dynamic vulcanization on the

Correspondence to: K. H. Seo (khseo@knu.ac.kr).

TABLE I
Basic Characteristics of Materials

Materials (trade name)	Characteristics	Source
Polyamide 6 (Ziamide, TP4407)	Density (g/cm ³): 1.12–1.15 Melting point (°C): 220–224 Moisture content (%): Max. 0.1	Zig sheng Industrial (Taiwan)
H-NBR (Zetpol 2010)	Relative viscosity: 2.70 ± 0.05 Specific gravity: 0.95 Bound acrylonitrile (%): 36.2 Mooney viscosity, ML 1+4 100°C: 85 Unsaturation: 4%	ZEON Corporation (Japan)
Peroxide (Luperox 101)	2,5-Dimethyl-2,5-di(tert-butyl peroxy)hexane	Elf Atochem (France)

blends was observed. The influence of peroxide on PA 6 was also analyzed.

EXPERIMENTAL

Materials

PA 6 used in this study was supplied by Zig Sheng Industrial (Taipei, Taiwan). Hydrogenated nitrile rubber (H-NBR) containing 36% bound acrylonitrile was provided by Zeon Corp. (Tokyo, Japan). The characteristics of the above materials are given in Table I. All materials were vacuum-dried at 60°C for 48 h to remove the moisture before use. Two antioxidants were also used to protect thermal degradation of PA 6 during mixing procedure.

Preparation of the blends and test sample and dynamic vulcanization

The blend ratios used in this study are presented in Table II and denoted by H0, H20, H40, H50, H60, H70, and H80. The designation of H means H-NBR and the numerical values denote the weight percentage (wt %) of H-NBR in the blends. PA 6/H-NBR blends were prepared with a Brabender plasti-coder® with a rotor speed of 100 rpm at 240°C, and the total mixing time was fixed at 8 min. PA 6 was first melted with antioxidants of 0.5 phr in the mixer, and then H-NBR was added after 1.5 min. Dynamic vulcanization was accomplished by adding LUPEROX 101 (peroxide) after 2.5 min when PA 6 and H-NBR was totally

mixed in the mixer, and the mixing was continued for 5.5 min (Table III). Test specimens were prepared by compression molding at 250°C under a force of 150 kg_f/cm². Appropriate specimens were cut from the sheets and used thereafter.

Characteristics

The mechanical properties such as tensile strength, modulus, and elongation at break were characterized according to the ASTM D638 test method using dumb-bell-shaped test specimens at a crosshead speed of 50 mm/min using the Universal Test Machine (Instron, model 4465). The permanent set of the blends was measured according to ASTM D412. The shore A type hardness of the samples was measured according to ASTM D2240. Oil resistance was measured by immersing the samples in ASTM #3 oil for 70 h at 150°C in accordance with ASTM D471. The changes in weight were recorded. The morphology of the samples was investigated by using the field emission scanning electron microscope (FE-SEM, Hitachi S-4300). The molded samples were fractured after freezing in liquid nitrogen for preventing the deformation of the sample during fracture, and fracture surface was sputter coated with gold before SEM observations. Differential scanning calorimeter (DuPont, DSC 10) was used to investigate heat of fusion (ΔH) of the blends. Melt flow index (MFI) of the blends was investigated by a melt flow indexer (DAVENPORT, MFI 10). The blends were placed in the capillary of the melt flow indexer at 250°C, and then the MFI change was measured. The load and cutting time were 2.16 kg and 60 s, respectively. Dynamic mechanical analysis of the blends was performed on DMA (Perkin-Elmer, dynamic

TABLE II
Composition of PA6/H-NBR Blends

Sample	H-NBR (wt %)	PA 6 (wt %)	Irganox1010 (phr)	Irgafos168 (phr)
H0	0	100	0.5	0.5
H20	20	80	0.5	0.5
H40	40	60	0.5	0.5
H50	50	50	0.5	0.5
H60	60	40	0.5	0.5
H70	70	30	0.5	0.5
H80	80	20	0.5	0.5

TABLE III
Composition of PA 6/H-NBR Blends with Peroxide Content

Sample	H-NBR (wt %)	PA 6 (wt %)	Peroxide (phr)		
Cured H50	50	50	1	2	3
Cured H60	60	40	1	2	3
Cured H70	70	30	1	2	3

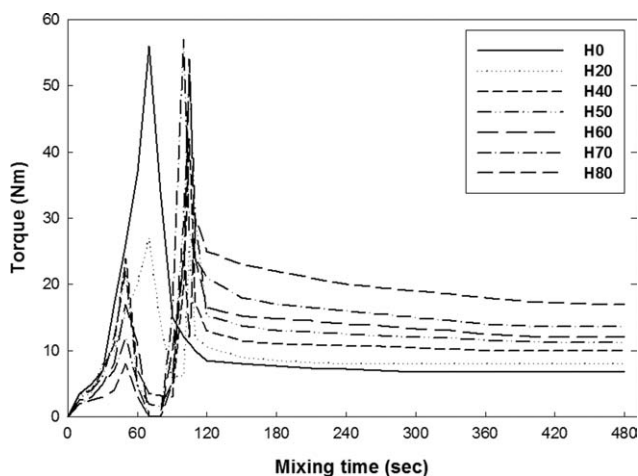


Figure 1 Variations of mixing torque during blending with respect to H-NBR content.

mechanical analyzer, N535). The experiments were carried out at a heating rate of $10^{\circ}\text{C}/\text{min}$ and a temperature range of -100 – 200°C . The storage modulus (G') and loss tangent ($\tan \delta$) were measured for each sample in this temperature range.

RESULTS AND DISCUSSION

Processing characteristics

Several researchers have used mixing torque during mixing procedures to analyze the processing characteristics of polymer blends.^{27,28} The processing characteristics of the blends were studied from the time-torque curves, shown in Figure 1.

All blends except H0 showed two peaks. The first peak is due to the introduction of unmolten PA 6 and decreases as PA 6 melts. The peak of the blends increases again with an addition of H-NBR and then comes down. The uniform torque value of the blends indicates a good level of mixing of the two polymers. After an addition of H-NBR, the torque values of the blends increase as H-NBR content increases. This is attributed to the high-melt viscosity of the H-NBR component compared to PA 6 as confirmed with Table IV showing the MFI values of PA 6/H-NBR blends. As H-NBR increased, MFI values decreased, suggesting that the melt viscosity of the blends increased.

TABLE IV
MFI Value of PA 6/H-NBR Blends

Sample	MFI (g/10 min)
H0	19.6
H20	14.3
H40	7.9
H50	7.5
H60	3.6
H70	2.2
H80	1.6

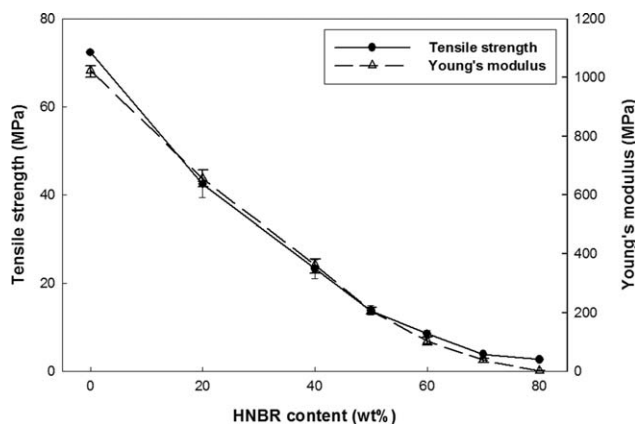


Figure 2 Tensile strength and Young's modulus of PA 6/H-NBR blends with respect to the HNBR content.

Physical properties

The properties of rubber–plastic blends are determined by the following factors: material properties of rubber and plastic phases, the blend ratio, the phase morphology, and the interaction between polymers.²⁹ Figure 2 shows the variation of tensile strength and Young's modulus with respect to H-NBR content. As H-NBR content increases, tensile strength and Young's modulus decrease. The strength of PA 6/H-NBR blends depends on the strength of the PA 6 phase. It has been observed that the heat of fusion value of the blends was decreased by incorporation of H-NBR as shown in Table V. This suggests the decrease of strength of the blends with increasing H-NBR.

Martuscelli et al.^{27,30,31} have shown that the spherulite growth of isotactic polypropylene (PP) in blends with rubber is hindered by the presence of the rubber phase. Hence, the observed decrease in tensile strength and Young's modulus with an increase in H-NBR content is due to the presence of the soft rubber phase and fall in crystallinity of the PA 6 phase.

Elongation at break and permanent set of the PA 6/H-NBR blends with respect to H-NBR content are presented in Figure 3. The elongation at break decreased with an addition of H-NBR and is found to be lowest for H50. This low value of the blends can be explained with the poor adhesion between

TABLE V
Heat of Fusion of PA 6/H-NBR Blends

Sample	Heat of fusion (J/g)
H0	63.7
H20	56.9
H40	42.8
H50	40.8
H60	34.1
H70	28.9
H80	18.3

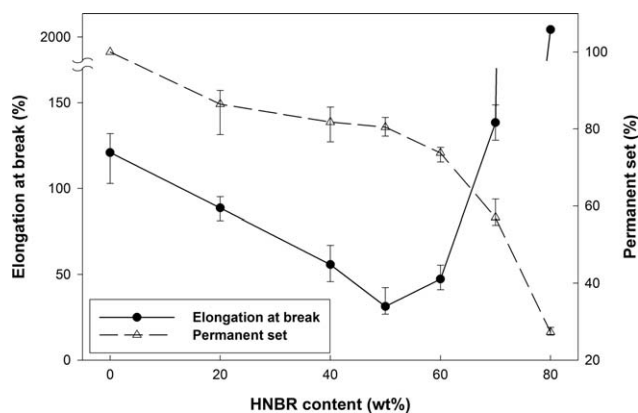


Figure 3 Elongation at break and permanent set of PA 6/H-NBR blends with respect to the H-NBR content.

the two phases in the blends. The poor adhesion can be confirmed by morphology observation. The large voids on the fractured surface where H-NBR domains had separated from the PA 6 matrix, and the smooth surface can explain that PA 6/H-NBR blends have poor interfacial adhesion. Thereafter, the elongation at break increases and is found to be highest for H80.

Kumar et al.³² have reported that the Nylon 6/NBR blend has the low value on elongation at break, and this is due to the poor adhesion between polymers. Duvall et al.³³ have investigated similar observations in nylon/PP blends. They have reported that the poor interfacial adhesion was evident from the large voids left on the fracture surface where the particles had separated from the matrix and smooth surfaces. The permanent set of the blends also decreases with an increase of H-NBR content. A sudden decrease above 60 wt % of H-NBR content is due to high recoverability of H-NBR phase after deformation.

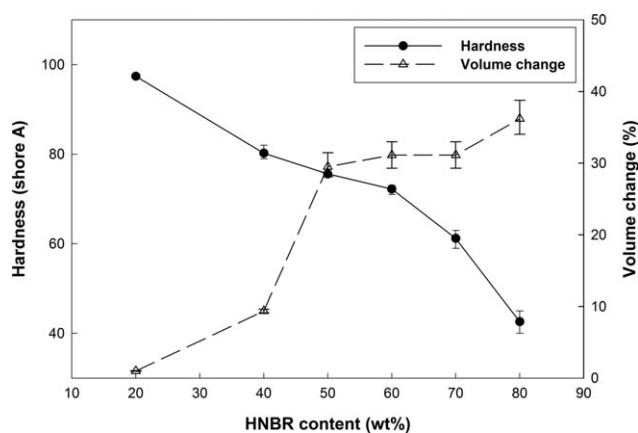


Figure 4 Hardness and volume change of PA 6/H-NBR blends with respect to the H-NBR content.

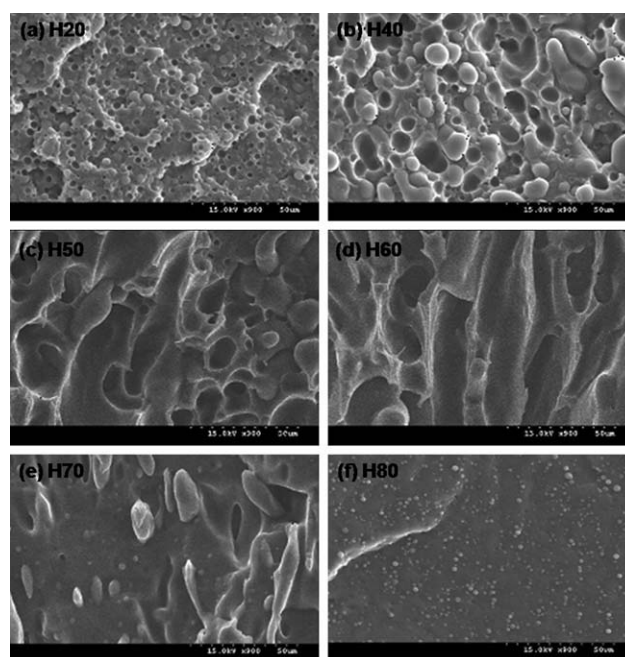


Figure 5 SEM micrographs of the fractured surface of the blends.

Figure 4 shows the hardness and volume change of the blends with respect to H-NBR content. It can be seen that increasing H-NBR content decreases the hardness and increases the swelling. Because the hardness is a surface property, it can be confirmed that PA 6 exists as a continuous phase less than 40 wt % of H-NBR, and more than 70 wt %, H-NBR exists as a continuous phase. The volume change of the samples increases with an increase of H-NBR, and a sudden increase from H50 is related to higher swelling effect resulting from the cocontinuous structure of the blends when compared with other blends having different ratios.

Morphology

It is reported in various literature that the important factors, which determine the morphology of polymer blends, are the blend ratio, melt viscosity of each component, shear stress, and so on.^{34,35} Figure 5(a–f) shows the SEM results of the fracture surface of the PA 6/H-NBR blends. The two phases can be distinguished from the results, suggesting that PA 6/H-NBR blends show an immiscible system. From (a) and (b), the holes are H-NBR domain in the PA 6 matrix, and the domain size increases with an increase in H-NBR content. This is attributed to coalescence of H-NBR domains. Many researchers have investigated the coalescent behavior of one of the components having higher concentration.^{35–38} The cocontinuous phase is observed in the blend ratio of 50/50 and 60/40 given to (c) and (d), and H-NBR

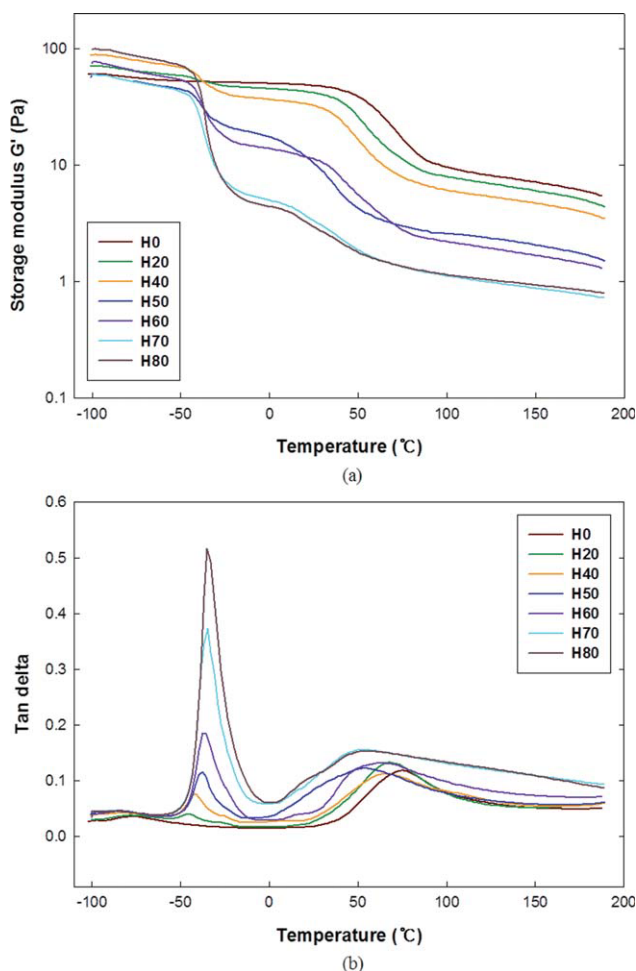


Figure 6 The storage modulus (G') (a) and $\tan \delta$ traces (b) of the blends. [Color figure can be viewed in the online issue, which is available at [wileyonlinelibrary.com](http://www.interscience.wiley.com).]

exists as a continuous phase in the blends when H-NBR increases beyond 70 wt %.

Dynamic mechanical property

Figure 6(a,b) shows temperature dependence of storage modulus (G') and loss tangent ($\tan \delta$) for the blends with respect to H-NBR content. As H-NBR content increases, G' is shifted downward and is in three distinct regions, H0–H40, H50–H60, and H70–H80. It can be inferred that the phase inversion from PA 6 phase to H-NBR phase through the cocontinuous phase, and it can be inferred that the PA 6 exists as a matrix up to a blend ratio of 40/60. The H-NBR exists as a matrix above a 70/30 blend composition. It is clear from the $\tan \delta$ curves that all blends except H0 show the following two main transitions in the temperature range of -100 – 200°C corresponding to the glass transition temperature (T_g) of H-NBR and PA 6, respectively, confirming two phase morphology of the blends. The change of $\tan \delta$ showing T_g was confirmed as seen in Figure 7, and this is attributed to

interaction due to the polarity of the two polymers. The broadening of $\tan \delta$ peaks of PA 6 with an increase of the H-NBR content may be attributed to loss of elasticity of PA 6 with an addition of H-NBR.

Influence of dynamic vulcanization

Variation of mixing torque

Figure 8(a–c) shows mixing torque values of the dynamically cured blends with respect to peroxide content. In all blends studied, torque values increase with an increase of peroxide content and increase with an increase of H-NBR content resulting from an increase of degree of crosslinking by peroxide. This is thought to be due to the increase of melt viscosity of H-NBR resulting from crosslinking.

Physical properties

The tensile strength and Young's modulus of cured blends with respect to peroxide content are given in Figure 9. Both tensile strength and Young's modulus decrease with an addition of peroxide content of 1.0 phr compared to uncured blends. It is reported that the mechanical properties such as tensile strength and Young's modulus increase if the crosslinking is progressed, but the results investigated in this study show opposite results. Mehrabzadeh et al.³⁹ observed that the peroxide can cause degradation of PA 6 during mixing in their study with Nylon 6/NBR blends. This is attributed to peroxide, which affected not only crosslinking of H-NBR but also PA 6, suggesting that peroxide can affect the PA 6.

It was found that the heat of fusion of cured blends with respect to peroxide content decreased with an addition of peroxide content of 1.0 phr. This seems to be due to hindrance of crystalline orientation of PA 6 resulting from crosslinking of PA 6, and this may be

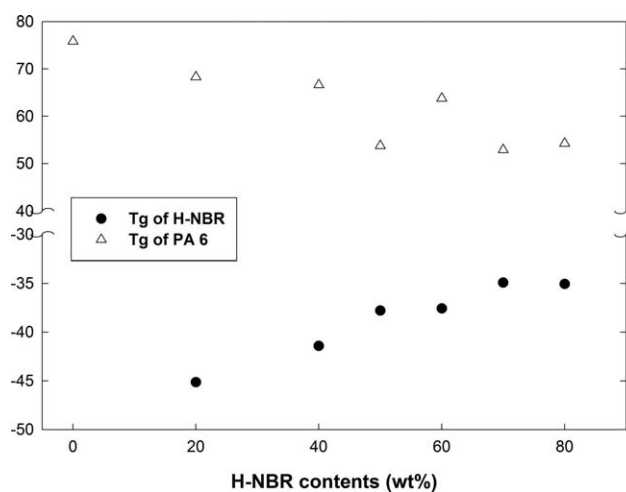


Figure 7 Change of T_g for the PA 6/H-NBR blends.

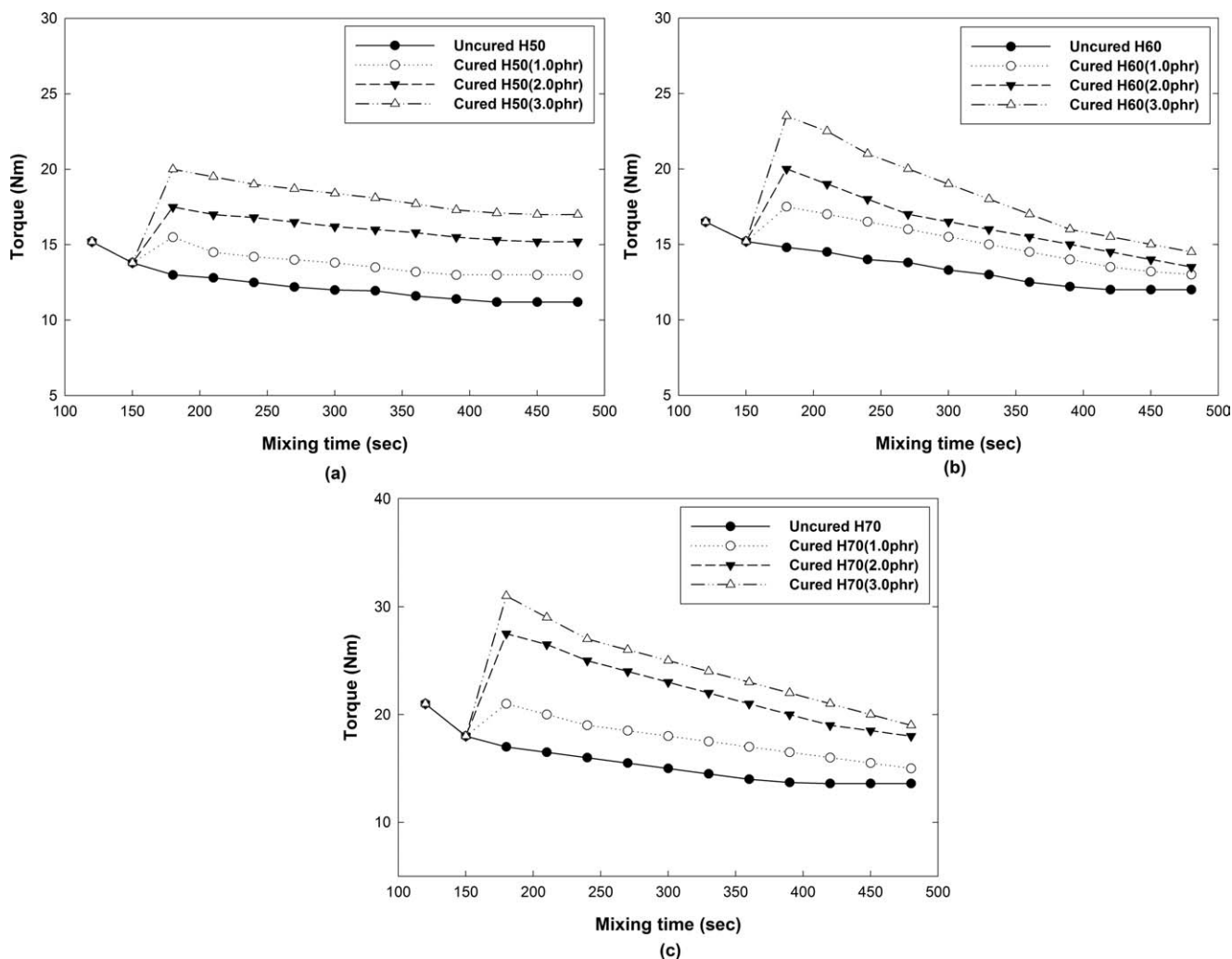


Figure 8 Variations of mixing torque during blending with respect to peroxide content (a) H50, (b) H60, and (c) H70.

related to the reduced mechanical properties of cured blends (not shown). Elongation at break and volume change of dynamically cured blends are given in Figure 10. A sudden increase of elongation at break in H70 is due to crosslinking of H-NBR existing as a continuous phase. It was also found that the volume change of cured blends was reduced due to crosslinking process. A 30/70 blend composition showed the maximum decrease, and this may be due to high-crosslinking effect of the H-NBR.

Morphology of the cured blends

Figure 11 shows the fracture surfaces of the cured blend with a ratio of 40/60. SEM micrographs obtained for other blend ratios, 50/50 and 30/70, were similar (not shown). Although it was found that the cocontinuous phases of H60 were changed with an addition of peroxide, a division of two phases could not be observed. This appears to be due to the fact that increased melt viscosity of the PA 6 by crosslinking could not form a continuous phase.

Dynamic mechanical property of the cured blends

Figure 12 shows temperature dependence of G' and $\tan \delta$ for the cured H60 blend with respect to peroxide content. It can be seen that the G' of the cured blend with a 1.0-phr peroxide is lower than that of an uncured blend. This is the same as the results of reduced mechanical properties as seen earlier. Above 2.0 phr peroxide, G' increased due to the increase of degree of crosslinking by peroxide. It can be seen that the decrease of $\tan \delta$ curves of H-NBR with over 2.0 phr peroxide is attributed to the increase of the elasticity by peroxide, and the increase of $\tan \delta$ curves of PA 6 is due to loss of elasticity by peroxide.

Effect of peroxide on PA 6

Mixing torque

Figure 13 shows the variation of mixing torque and the MFI of the PA 6 with respect to peroxide content. The torque values increase with an increase of peroxide content, and this is attributed to the increase of the

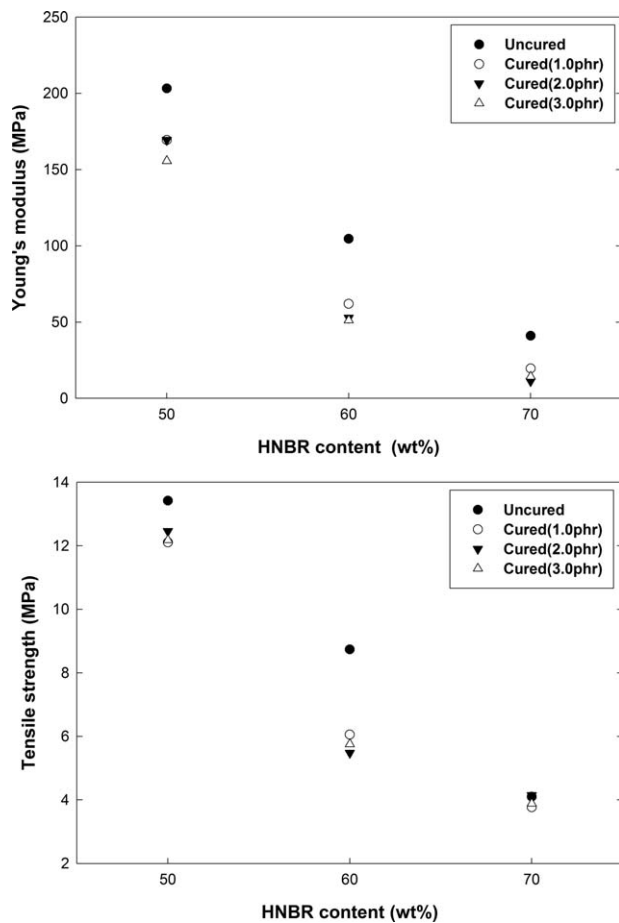


Figure 9 Tensile strength and Young's modulus of dynamically cured PA 6/H-NBR blends.

melt viscosity of the PA 6 by the peroxide as confirmed in MFI values of PA 6. As peroxide content increased, MFI values decreased, suggesting that the melt viscosity of the PA 6 increased. It can be seen that the PA 6 was almost fully crosslinked by a peroxide content of less than 1.0 phr. In addition, this result was related to the reason that PA 6 could not exist as a continuous phase of the blends with ratios of 50/50 and 40/60 due to increased melt viscosity as seen in morphology observation.

Physical and dynamic mechanical properties

The Young's modulus and elongation at break of PA 6 with respect to peroxide content are shown in Figure 14. The Young's modulus decreased with less than 1.0 phr of peroxide, and this behavior can be confirmed with a heat of fusion value of PA 6, showing that reduction of the heat of fusion values with an addition of peroxide (not shown). A sudden decrease of the elongation at break may be due to the increase of stiffness of PA6 resulting from the crosslinking process. In addition, it was found that the $\tan \delta$ of PA6 increased with an addition of the

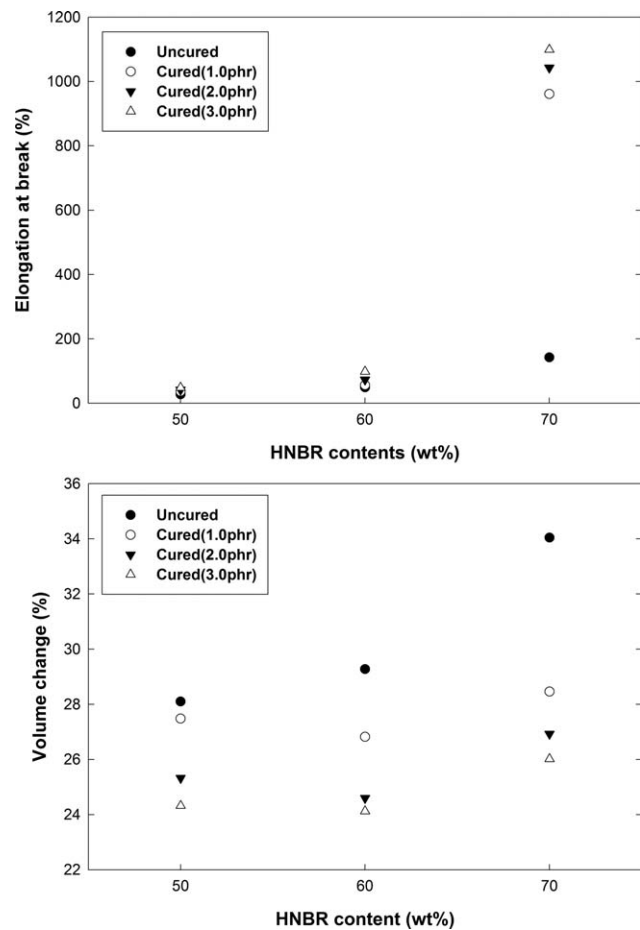


Figure 10 Elongation at break and volume change of dynamically cured PA 6/H-NBR blends.

peroxide. It can be seen that adding peroxide on PA 6 caused a loss of elastic property of PA 6, resulting in reduction of mechanical properties (not shown).

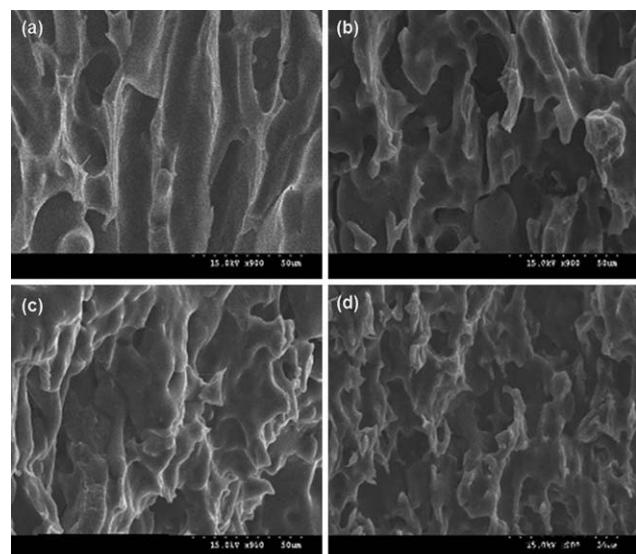


Figure 11 SEM micrographs of the fracture surface of the cured blends at the ratio 40/60 (a) 0 (b) 1.0, (c) 2.0, and (d) 3.0 phr.

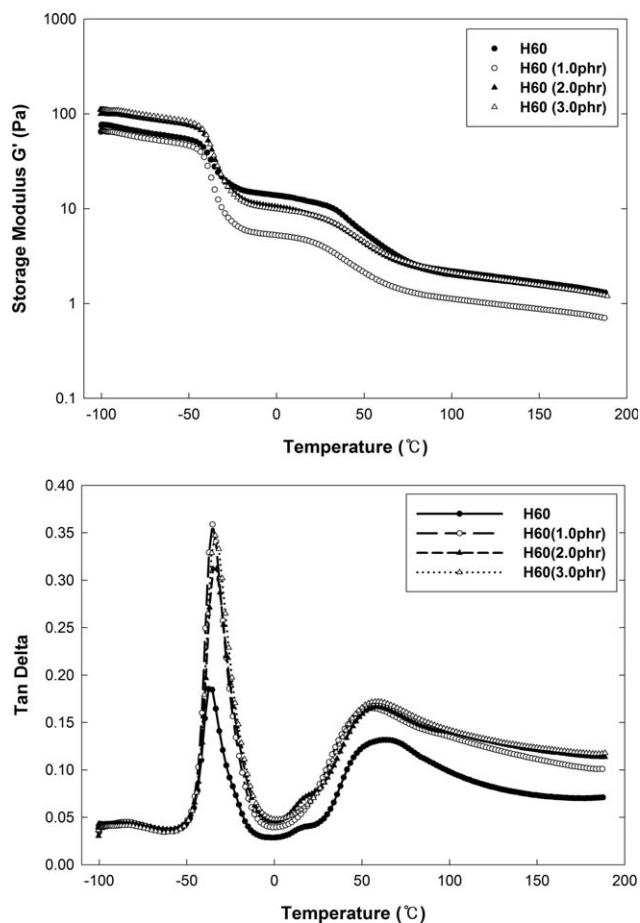


Figure 12 The storage modulus (G') and $\tan \delta$ traces of the cured H60 blends.

CONCLUSIONS

The mixing torque of the PA 6/H-NBR blends increased with an addition of amorphous H-NBR having high-melt viscosity, and mechanical properties decreased due to the presence of the soft H-NBR phase and reduced crystallinity of the blends. The two distinguished phases were confirmed from the morphology observation. The PA 6 exists as a continuous phase in the blends of less than 40 wt % of H-NBR content, and H-NBR exists as a continuous phase in the blends when H-NBR increases beyond 70 wt %. It was confirmed that the storage modulus (G') decreased with an increase of H-NBR, suggesting that phase inversion from PA6 phase to H-NBR phase through cocontinuous phase from the DMA results. It was found that the mechanical properties such as tensile strength and Young's modulus of the cured blends were lower than those of uncured blends, suggesting that peroxide can affect PA 6 as well as H-NBR as a crosslinker, and the elongation, hardness, and swelling behavior were enhanced by crosslinking. It was found that PA 6 could not make a continuous phase at ratios of 50/50 and 40/60 due

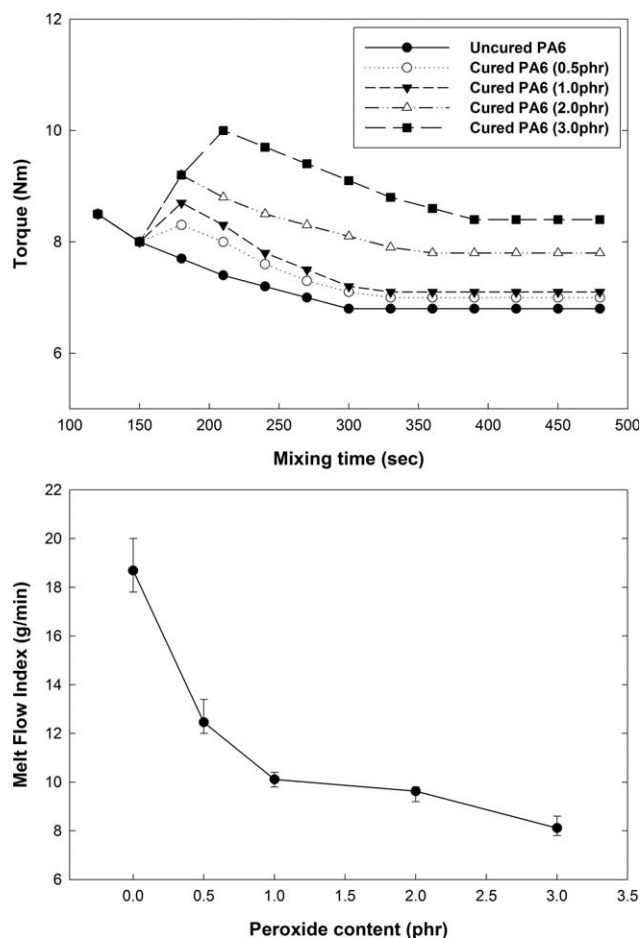


Figure 13 Variations of mixing torque and melt flow index during mixing of PA 6 with respect to peroxide content.

to increased melt viscosity of PA 6 by crosslinking. From the results of the influence of peroxide on PA 6, the peroxide increased mixing torque, suggesting that melt viscosity of PA 6 was increased by peroxide.

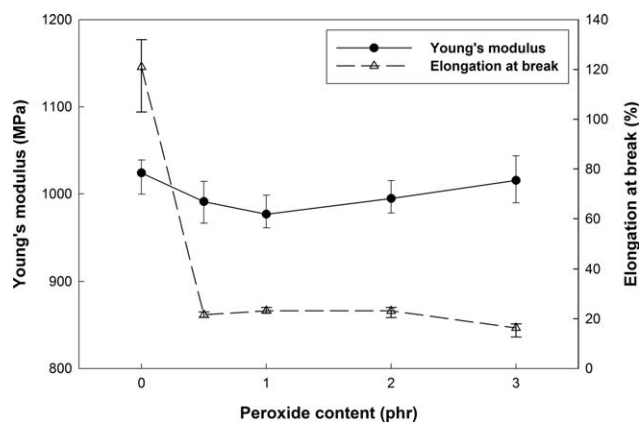


Figure 14 Effect of peroxide content on Young's modulus and elongation at break of PA 6.

References

1. Utracki, L. A. *Commercial Polymer Blends*; Chapman & Hall: London, 1998.
2. Paul, D. R.; Bucknall, C. B. *Polymer Blends*; Wiley: New Jersey, 1999.
3. Paul, D. R.; Newman, S. *Polymer Blends*; Academic Press: New York, 1978.
4. Olabisi, O.; Robeson, L. M.; Shaw, M. T. *Polymer-Polymer Miscibility*; Academic Press: New York, 1978.
5. Xanthos, M. *Polym Eng Sci* 1998, 28, 1932.
6. Thomas, S.; Prud'homme, R. E. *Polymer* 1992, 33, 4260.
7. Liao, F. S.; Su, A. C.; Tzu-chien, X.; Hsu, J. *J Polym* 1994, 35, 2579.
8. Inoue, T.; Suzuki, T. *J Appl Polym Sci* 1995, 56, 1113.
9. Mehrabzadeh, M.; Delfan, N. *J Appl Polym Sci* 2000, 77, 2057.
10. Holden, G. *J Elastoplastic* 1970, 2, 234.
11. Ferrara, R. *J Rubber Age* 1976, 99, 53.
12. Fischer, W. K. U.S. Pat, 3,758,643 (1973).
13. Fischer, W. K. U.S. Pat, 3,835,201 (1974).
14. Fischer, W. K. U.S. Pat, 3,862,106 (1975).
15. Carman, C. J.; Batiuk, M.; Harman, B. M. U.S. Pat, 4,046,840 (1977).
16. Gessler, M. U.S. Pat, 3,037,954 (1962).
17. Fischer, W. K. U. S. Pat, 3,758,648 (1973).
18. Coran, A. Y.; Patel, R. *Rubber Chem Technol* 1980, 53, 141.
19. Abdou-Sabet, S.; Patel, R. *Rubber Chem Technol* 1991, 64, 769.
20. Huang, H.; Yang, J.; Liu, X.; Zhang, Y. *Eur Polym J* 2002, 38, 857.
21. Wu, S. *Polymer* 1985, 26, 1855.
22. Margolina, A.; Wu, S. *Polymer* 1988, 29, 2170.
23. Fukui, T.; Kikuchi, Y.; Inoue, T. *Polymer* 1991, 32, 2367.
24. Takeda, Y.; Keskkula, H.; Paul, D. R. *Polymer* 1992, 33, 3173.
25. Bhowmick, A. K.; Stephens, H. L. *Handbook of Elastomers*; Marcel Dekker Inc.: New York, 1988; p 785.
26. Huang, H.; Ikehara, T.; Nishi, T. *J Appl Polym Sci* 2003, 90, 1242.
27. George, S.; Joseph, R.; Thomas, S.; Varughese, K. T. *Polymer* 1995, 36, 4405.
28. Dagli, S. S.; Xanthos, M.; Biesenberger, J. A. *Polym Eng Sci* 1994, 34, 1720.
29. Coran, A. Y. *Handbook of Elastomers—New Development and Technology*; Bhowmick, A. K., Stephens, H. L., Eds.; Marcel Dekker: New York, 1988; p 249.
30. George, S.; Varughese, K. T.; Thomas, S. *Polymer* 2000, 41, 5485.
31. Martusceli, E.; Silvestre, C.; Abate, G. *Polymer* 1982, 23, 229.
32. Kumar, C. R.; George, K. E.; Thomas, S. *J Appl Polym Sci* 1996, 61, 2383.
33. Duvall, J.; Selliti, C.; Topolkaev, V.; Hiltner, A.; Baer, E.; Myers, C. *Polymer* 1994, 35, 3948.
34. Shonaike, G. O.; Simon, G. P. *Polymer Blends and Alloys*; Marcel Dekker: New York; 1999.
35. Danesi, S.; Porter, R. S. *Polymer* 1978, 19, 448.
36. Thomas, S.; Kuriakose, B.; Gupta, B. R.; De, S. K. *J Mater Sci* 1986, 21, 711.
37. Hheikens, D.; Barentsen, W. *Polymer* 1977, 18, 69.
38. Thomas, S.; Gupta, B. R.; De, S. K. *J Vinyl Technol* 1987, 9, 71.
39. Mehrabzadeh, M.; Delfan, N. *J Appl Polym Sci* 2000, 77, 2057.